Use of Computed Tomography-Guided Percutaneous Biopsy of Invasive Non-Mucinous Lung Adenocarcinoma to Predict the Degree of Histological Differentiation

Dehao Liu[1]*, Lichun Chen[2]* iD, Xiaoping Wang[1], Yikai Lin[1] and Jianwei Gu[1]

[1]Department of Radiology, The First Affiliated Hospital of Xiamen University, Xiamen, China.
[2]Department of Radiology, Xiamen Hospital of Traditional Chinese Medicine, Xiamen, China.

ABSTRACT

BACKGROUND: The International Association for the Study of Lung Cancer (IASLC) published a grading system for invasive pulmonary adenocarcinoma that is closely associated with prognosis. This study aimed to investigate the accuracy of computed tomography (CT)-guided biopsy specimen grading and surgery-guided grading systems for detecting invasive non-mucinous lung adenocarcinoma and to determine whether CT-guided biopsy can predict the degree of histological differentiation.

METHODS: In total, 130 patients with invasive non-mucinous lung adenocarcinoma who underwent CT-guided biopsy before surgical excision were retrospectively studied. Biopsy and surgical specimen pathologies were compared. Grading was performed according to different subtypes proposed by the International Association for the Study of Lung Cancer. Sensitivity, specificity, positive and negative predictive values (PPV/NPV), and accuracy were calculated for each subtype and grade.

RESULTS: The concordance rates of biopsy and surgical pathology subtypes and grades were 73.1% and 72.3%, respectively. Sensitivity, specificity, PPV, NPV, and accuracy of grade 3 were 54.8%, 100%, 100%, 87.6%, and 89.2%, respectively. Pathology grades were primarily discrepant with respect to two aspects of biopsy and surgical samples in the same patient. First, the biopsy and surgical specimen pathology findings indicated lepidic and acinar subtypes as the main subtypes in the same patient, respectively. Second, biopsy specimen histology did not find solid types; however, >20% of solid subtypes were identified in surgical pathology samples in the same patient.

CONCLUSIONS: The preoperative CT-guided biopsy specimen grading system showed relatively high accuracy and could predict the prognosis of invasive non-mucinous lung adenocarcinoma.

KEYWORDS: Accuracy, biopsy, grading system, histological subtype, lung adenocarcinoma

Introduction

The GLOBOCAN 2018 database indicates that lung cancer represents the most frequent cause of cancer-related death worldwide. Lung cancer ranked first in men and second in women in terms of the number of new cancer cases and number of deaths 2018.[1] With the wide clinical application of low-dose computed tomography (CT), the detection rate for early lung cancer is increasing. Among lung cancers, lung adenocarcinoma is the most common, accounting for approximately 40% of all lung cancers. Moreover, it is an architecturally heterogeneous tumor, consisting of multiple components, and there is a risk of recurrence, even if it is treated and excised at an early stage.[2,3]

In 2011, the International Association for the Study of Lung Cancer (IASLC), American Thoracic Society (ATS), and European Respiratory Society (ERS) set forth a new classification for lung adenocarcinoma. Under this classification, lung adenocarcinoma is divided into the following five subtypes: lepidic (LEP), acinar (ACI), papillary (PAP), micropapillary (MIP), and solid (SOL). This classification also highlights that the MIP subtype, similar to the SOL subtype, has poor prognosis, and MIP has been found to be prone to metastasis.[3] In 2020, the IASLC proposed a grading system for invasive pulmonary adenocarcinoma.[4] Both of these systems are listed in the 2015 World Health Organization (WHO) classification and the 2021 WHO classification of lung tumors.[5,6] In 2020, the IASLC also mentioned that a cribriform pattern is a high-grade pattern of the ACI subtype.[4] Currently, a cribriform pattern with high mitotic activity, tumor necrosis, and lymphovascular invasion can predict local lymph node metastasis.[7] Patients with lung adenocarcinoma with a cribriform pattern have a poor prognosis, similar to patients with MIP and SOL subtypes.[8] Therefore, it is classified as a high-grade type.

The histological subtype of lung adenocarcinoma is a prognostic factor, and treatment can be planned based on the histological subtype and grade. This includes the determination

---

* Dehao Liu and Lichun Chen contribute equally, and should be regarded as co-first authors.

of the ablation range, selection of the surgical resection method, stereotactic body radiation therapy dose, or volume escalation.[9-11] The subtype and grade of lung adenocarcinoma can be obtained via CT-guided biopsy prior to tumor treatment. Nonetheless, the accuracy rate of histological subtype determination has not been compared between CT-guided biopsy specimens and final surgical specimens. Therefore, this retrospective study aimed to compare the accuracy of grade determination by histopathological examination of CT-guided biopsy specimens as compared with that of surgically resected specimens in patients with lung adenocarcinoma.

Methods

Patients

A total of 1093 patients with lung lesions who underwent CT-guided percutaneous biopsy at the First Hosptial of Xiamen University between February 2019 and February 2021 were retrospectively enrolled. Subsequently, 154 patients underwent lung surgery. Patients diagnosed with invasive non-mucinous lung adenocarcinoma were enrolled in the study. Overall, 130 patients were retrospectively analyzed (Figure 1).

The inclusion criteria for this study were as follows: (1) Biopsy pathology and surgical pathology were derived from the same lesion; (2) no treatment, including chemotherapy, radiotherapy, and targeted therapy, was performed before CT-guided biopsy and lung resection; (3) the results of both biopsy pathology and surgical pathology indicated subtypes of invasive non-mucinous lung adenocarcinoma; (4) the interval between the biopsy puncture and surgery was < 180 days; and (5) all lung adenocarcinoma patients were in clinical stages I–III. This study was approved by the ethics committee of the First Hospital of Xiamen University (approval number: 2022013). All patients provided signed informed consent forms prior to biopsy.

CT-guided biopsy

The CT-guided biopsy procedure was performed by experienced interventional radiologists. According to the lesion displayed on the CT image before puncture, we evaluated the feasibility and safety of biopsy, and used the shortest puncture path while avoiding underlying important anatomical structures, such as blood vessels, the skeleton, and the heart. Under sterile conditions, and using local anesthesia with lidocaine, a core needle biopsy was performed under CT guidance. We use a 17-G or 19-G coaxial guided biopsy needle and an 18-G (CareFusion, San Diego, CA, USA) or a 20-G automatic biopsy needle (Argon Medical Devices, Athens, TX, USA) was used. The size of the biopsy tissue was recorded (including biopsy needle gauge, number of biopsy tissue and length of each biopsy tissue for each patient).

Histopathological subtypes

Pathological examination of tissue samples obtained by biopsy or during surgery was performed independently by experienced pathologists. The subtypes of invasive non-mucinous lung adenocarcinoma were defined according to IASLC/ATS/ERS guidelines 2011.[3] The subtypes of invasive non-mucinous lung adenocarcinoma included LEP, ACI, PAP, MIP, and SOL. The MIP-SOL group implied that the invasive non-mucinous lung adenocarcinoma contained MIP, SOL, or both MIP and SOL subtypes. The non-MIP-SOL group included the LEP, ACI, and PAP subtypes. The grades of invasive non-mucinous lung adenocarcinoma are based on the ratio of predominant patterns (LEP, ACI, PAP, MIP, SOL) to high-grade patterns (MIP, SOL, cribriform, or complex glandular) (Figure 2).

The IASLC published a grading system for invasive pulmonary adenocarcinoma in 2020,[4] defined as follows:

1. Grade 1 (well-differentiated): LEP predominant, with none or less than 20% high-grade patterns.
2. Grade 2 (moderately differentiated): ACI or PAP predominant, with none or less than 20% high-grade patterns.
3. Grade 3 (poorly differentiated): Any tumor with 20% or more high-grade patterns.

We categorized the pathology results of the biopsy and surgical specimens as grade 1 to grade 3. A total of 130 patients were divided into two groups on the basis of consistency of pathological grading between the biopsy and surgical samples. If the pathological grading of the biopsy sample was consistent with that of the surgical samples in the same patient, they were classified as one group, and if the pathological grading of the biopsy sample was inconsistent with that of the surgical samples in the same patient, they were classified as another group. The invasive non-mucinous lung adenocarcinoma subtype determined by pathological examination of the surgical specimen was considered to be the gold standard.

Data collection

Clinical data of patients, including age, sex, imaging morphology, tumor location, tumor size, biopsy specimen size, biopsy time, biopsy needle specification, biopsy complications, and biopsy and surgical pathology subtypes of lung adenocarcinoma, were obtained from medical records. Biopsy time was determined as the time lapsed from the CT scan that was performed to locate the lesion to the CT scan that was repeated after sampling. Imaging morphology was divided into pure ground-glass opacities, part-solid, and solid. The presence of cavities in the lesion and pleural involvement on CT images were also recorded.

Complications of CT-guided biopsy included pneumothorax, alveolar hemorrhage (with or without hemoptysis), air
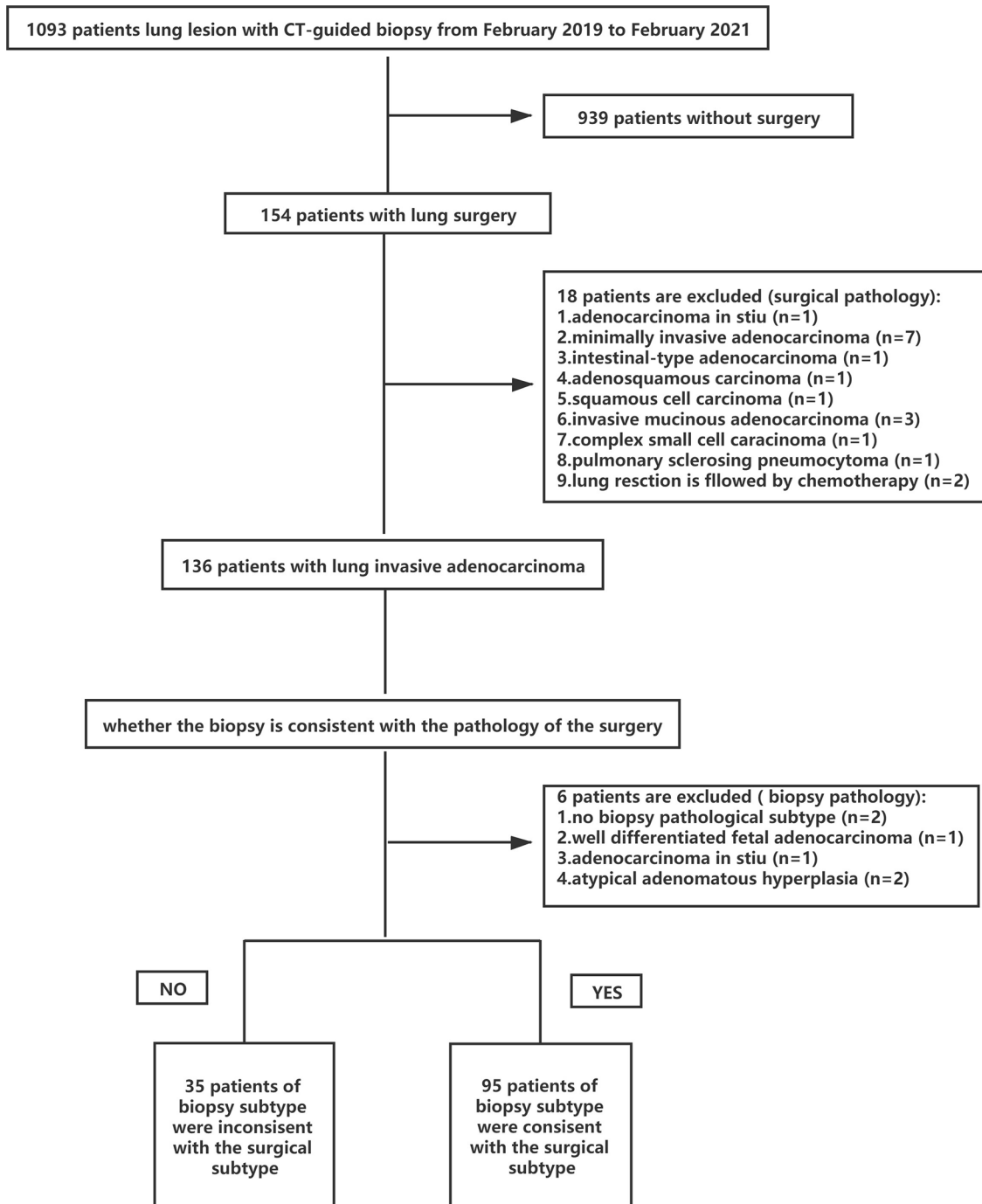
Figure 1. Flowchart of screening of 130 cases of invasive non-mucinous lung adenocarcinoma. CT indicates computed tomography.

embolism, and death. Depending on the severity of the pneumothorax, we will determine whether to use catheter drainage. Patients with pneumothorax (<30%) did not require treatment and could be self-absorbed, whereas a tube had to be placed in patients with >30% pneumothoraxes to facilitate drainage.

Statistical analysis

The normality of measurement data was first tested. To compare differences between the groups, the *t*-test was subsequently applied to normally distributed data, whereas the rank-sum test was used for non-normally distributed data. The chi-square test was used to compare categorical variables. Sensitivity, specificity, positive predictive value (PPV), negative predictive value (NPV), accuracy, and concordance were calculated (the formulas are presented below). *P*-values < 0.05 were considered to be indicative of statistical significance. Statistical analysis was performed using SPSS software version 26.0 (SPSS, Chicago, IL, USA).
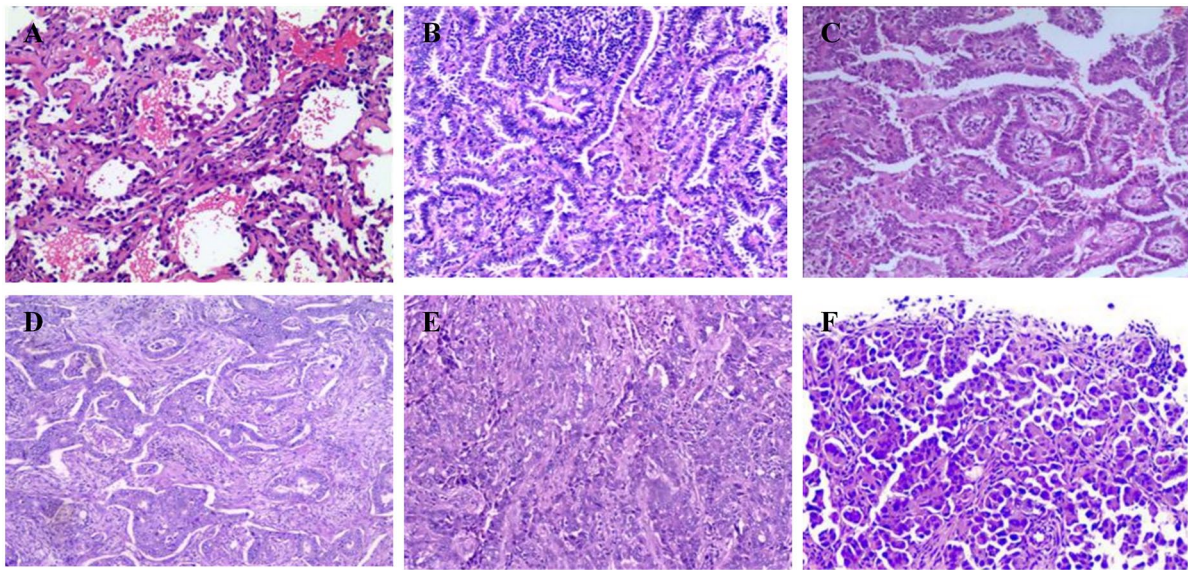
Figure 2. Histologic examples of lung adenocarcinoma subtypes: the LEP (A), ACI (B), PAP (C), cribriform (D), SOL (E) and MIP (F) are predominant patterns in histologic specimens (HE, magnification, ×100).
ACI indicates acinar; LEP, lepidic; MIP, micropapillary; PAP, papillary; SOL, solid; HE, hematoxylin-eosin staining.

Formulas

$$Specificity = \frac{true\ negative}{false\ postive + true\ negative} \times 100\%$$

$$Positive-predictive\ value\left(PPV\right) = \frac{true\ postive}{true\ postive + false\ postive} \times 100\%$$

$$Negative-predictive\ value\left(NPV\right) = \frac{true\ negative}{true\ negative + false\ postive} \times 100\%$$

$$Accuracy = \frac{true\ postive + true\ negative}{true\ postive + false\ postive + true\ negative + false\ negative} \times 100\%$$

$$Concordance = \frac{true\ postive}{true\ postive + false\ postive + true\ negative + false\ negative} \times 100\%$$

Results

Characteristics of patients in the study population

Patient characteristics are detailed in Table 1. The median patient age was 61 years, with a male-to-female ratio of 1:1.2 (59/71). The main morphological feature was a solid mass or nodule (73.4%). The proportion of tumor distribution in each lobe was as follows: right upper lobe, 33.8%; right middle lobe, 6.9%; right lower lobe, 17.7%; left upper lobe, 26.2%; left lower lobe, 15.4%. The median diameter of tumors was approximately 2 cm (range: 0.7-6.8 cm). Of the tumors, 43.8% had a diameter of 1-2 cm. The length of the biopsy sample was approximately 0.9 cm (range: 0.3-5.2 cm). The puncture time was approximately 14 min. We used 18-G and 20-G biopsy needles in 64.6% and 35.4% of cases, respectively. The median time interval between biopsy and surgery was 23 days (range: 5-156 days).

Clinical diagnostic efficiency of CT-guided biopsy

The predominant pathological subtypes determined from CT-guided biopsy and surgical specimens are compared in Table 2. The patients were divided into three groups according to the ratio of predominant patterns to high-grade patterns, as shown in Supplemental Appendix Table A1. In biopsy samples and surgical samples taken from the same patients, the concordance rate of overall pathological subtype and grade was 73.1% and 72.3%, respectively (Supplemental Appendix Table A2). The sensitivity, specificity, NPV, PPV, and accuracy of invasive non-mucinous lung adenocarcinoma subtypes and grades were calculated using the formulas (Table 3). The biopsy-based pathological subtype showed that the accuracy, sensitivity, specificity, PPV, and NPV of MIP (SOL) were 98.5% (96.2%), 66.7% (76.9), 99.2% (99.1%), 66.7% (90.9%), and 99.2% (97.5%), respectively. Among the three groups, the

Table 1. Patients characteristics.

VARIABLES	VALUE
All patients	130
Age (years)	
Median (range)	61 (9-82)
Sex (male/female)	59/71
Imaging morphology	
GGO (%)	17 (13.1)
Part solid (%)	17 (13.1)
Solid (%)	96 (73.8)
Cavity (%)	13 (10)
Pleural involvement (%)	42 (32.3)
Tumor location	
Right upper lobe (%)	44 (33.8)
Right middle lobe (%)	9 (6.9)
Right lower lobe (%)	23 (17.7)
Left upper lobe (%)	34 (26.2)
Left lower lobe (%)	20 (15.4)
Tumor size (cm)	
Median (range)	2 (0.7-6.8)
≤1.0 (%)	13 (10)
1.0>; ≤2.0 (%)	57 (43.8)
2.0>; ≤3.0 (%)	29 (22.3)
>3.0 (%)	31 (23.4)
Biopsy specimen length (cm)	
Median (range)	0.9 (0.3-5.2)
≤0.5 (%)	29 (22.3)
>0.5 ≤1.0 (%)	58 (44.6)
>1.0 ≤1.5 (%)	29 (22.3)
>1.5 (%)	14 (10.8)
Puncture biopsy time (min)	
Median (range)	14 (3-46)
Biopsy needle gauge	
18G (%)	84 (64.6)
20G (%)	46 (35.4)
Median time(from biopsy to surgery day)	
Median (range)	23 (5-156)

GGO, ground-glass opacity.

highest accuracy rate (89.2%) was obtained for grade 3, followed by grade 1 (77.7%) and grade 2 (81.5%). The PPV arranged from high to low in the following order: grade 3 (100%), grade 2 (81.2%), and grade 1 (38.9%). The sensitivity was in the following order: grade 1 (87.5%), grade 2 (75.9%), and grade 3 (54.8%).

Complications

As shown in Table 2, 72.3% (94/130) of patients had some degree of alveolar hemorrhage (with or without hemoptysis) during the course of biopsy. This included 22.3% (29/130) of patients with hemoptysis and 50% (65/130) of patients with a small amount of needle hemorrhage does not cause hemoptysis. Additionally, 19.2% (25/130) of patients had a small amount of pneumothorax; however, no patient required chest tube insertion. There were no air emboli or deaths (Supplemental Appendix Fig A1).

Variables associated with consistency of the grading system

The pathological grading of the biopsy sample was consistent with that of the surgical samples in 94 patients, and the pathological grading of the biopsy sample was inconsistent with that of the surgical samples in 36 patients. This is shown in Table 4.

We evaluated variables that could affect concordance between the biopsy and surgical specimen pathologies. These variables included age, sex, imaging morphology, tumor size, biopsy specimen size, biopsy needle gauge, and the pathological subgroup determined from CT-guided biopsy (Table 4).

The differences among the groups were statistically significant for the CT-guided biopsy subgroup ($P < 0.001$). We analyzed 36 patients with inconsistent biopsy and surgical specimen gradings (Table 5). Gradings were found to be inconsistent in two respects: the proportion of the predominant pattern and inclusion or exclusion of high-grade patterns. In 47.2% of discrepant cases, the biopsy showed that LEP was the main subtype, while surgical pathology showed that ACI was the main subtype. In 22.2% of discrepant cases, the biopsy histopathology did not report more than 20% SOL (Figure 3).

There was no significant difference in age, sex, imaging morphology, tumor size, biopsy specimen size, or biopsy needle gauge among the different groups.

Discussion

This study compared the consistency between biopsy-based and surgical specimen-based histopathology in cases with invasive lung adenocarcinoma. In 2015, the WHO defined the complex glandular pattern as a high-grade pattern of the ACI subtype, rather than as a new subtype. Thus, we compared five adenocarcinoma subtypes, not including the complex glandular pattern. Then, biopsy and surgical histopathologies were graded according to different subtypes.

Table 2. Compare pathologic subtypes of CT-guided biopsy and surgery, and CT-guided biopsy complications.

		PREDOMINANT PATHOLOGIC SUBTYPE OF SURGERY SPECIMENS						CT-GUIDED BIOPSY COMPLICATIONS		
		LEP	ACI	PAP	MIP	SOL	MIP-SOL	PNEUMOTHORAX	ALVEOLAR HEMORRHAGE	HEMOPTYSIS
Predominant pathologic subtype of biopsy specimens	LEP	15	17	3	0	1	3	4	25	7
	ACI	2	64	5	1	2	27	14	54	18
	PAP	1	1	4	0	0	2	3	4	1
	MIP	0	1	0	2	0	3	1	3	0
	SOL	0	1	0	0	10	11	3	8	3
	Total	18	84	12	3	13	46	25	94	29

Abbreviations: ACI, acinar; CT, computed tomography; LEP, lepidic; MIP, micropapillary; PAP, papillary; SOL, solid.

Table 3. Evaluate the clinical diagnostic efficiency CT-guided biopsy.

VARIABLES	LEP	ACI	PAP	MIP	SOL	MIP-SOL	GRADE 1	GRADE 2	GRADE 3
Sensitivity (%)	83.3	76.2	33.3	66.7	76.9	41.3	87.5	75.9	54.8
Specificity (%)	81.3	78.3	98.3	99.2	99.1	97.6	80.7	70.2	100
NPV (%)	96.8	64.3	92.8	99.2	97.5	75.2	97.7	62.3	87.6
PPV (%)	41.7	86.5	66.7	66.7	90.9	90.5	38.9	81.2	100
Accuracy (%)	81.5	76.9	92.3	98.5	96.2	77.7	81.5	73.8	89.2

Abbreviations: ACI, acinar; CT, computed tomography; LEP, lepidic; MIP, micropapillary; MIP-SOL, micropapillary-solid; NPV, negative predictive value; PAP, papillary; PPV, positive predictive value; SOL, solid.

Table 4. Variables associated with consistency of pathologic.

VARIABLES		CONSISTENT GROUP (N=94)		INCONSISTENT GROUP (N=36)		P VALUE
Age (years)	Median (range)	60 (29-76)	Median (range)	63 (39-77)		0.272
Sex	Men	41	Men	18		
	Women	53	Women	18		0.513
Imaging morphology	GGO	11	GGO	6		
	Part-solid	11	Part-solid	6		
	Solid	72	Solid	25		0.515
Tumor size (cm)	Median (range)	1.8 (0.8-6.8)	Median (range)	2.3 (0.7-6.7)		0.265
Biopsy specimen size (cm)	Median (range)	0.8 (0.3-5.2)	Median (range)	1.0 (0.5-3.5)		0.720
Biopsy needle gauge	18G	64	18G	20		
	20G	30	20G	16		0.181
Pathologic subgroup of CT-guided biopsy	LEP	14	LEP	22		
	ACI	61	ACI	13		
	PAP	5	PAP	1		
	MIP	3	MIP	0		
	SOL	11	SOL	0		<0.001**

Abbreviations: ACI, acinar; CT, computed tomography; LEP, lepidic; MIP, micropapillary; PAP, papillary; SOL, solid; GGO, ground-glass opacity.
**Statistically significant after accounting for multiple comparisons ($P < 0.01$).

Table 5. Analyzed grade inconsistent of pathologic of CT-guided biopsy samples and surgery samples for 36 patients.

	PREDOMINANT PATTERN OF CT-GUIDED BIOPSY	PREDOMINANT PATTERN OF SURGERY	PATIENTS (N = 36) (%)
The proportion of predominant pattern is different	LEP	ACI	17 (47.2)
	ACI	LEP	2 (5.6)
	LEP	PAP	3 (8.3)
Whether high-grade patterns is included	No	Yes, SOL	8 (22.2)
	No	Yes, MIP	1 (2.8)
	No	Yes, SOL + MIP	2 (5.6)
	No	Yes, SOL + Cribriform	2 (5.6)
	No	Yes, MIP + Cribriform	1 (2.8)

Abbreviations: ACI, acinar; CT, computed tomography; LEP, lepidic; MIP, micropapillary; PAP, papillary; SOL, solid.
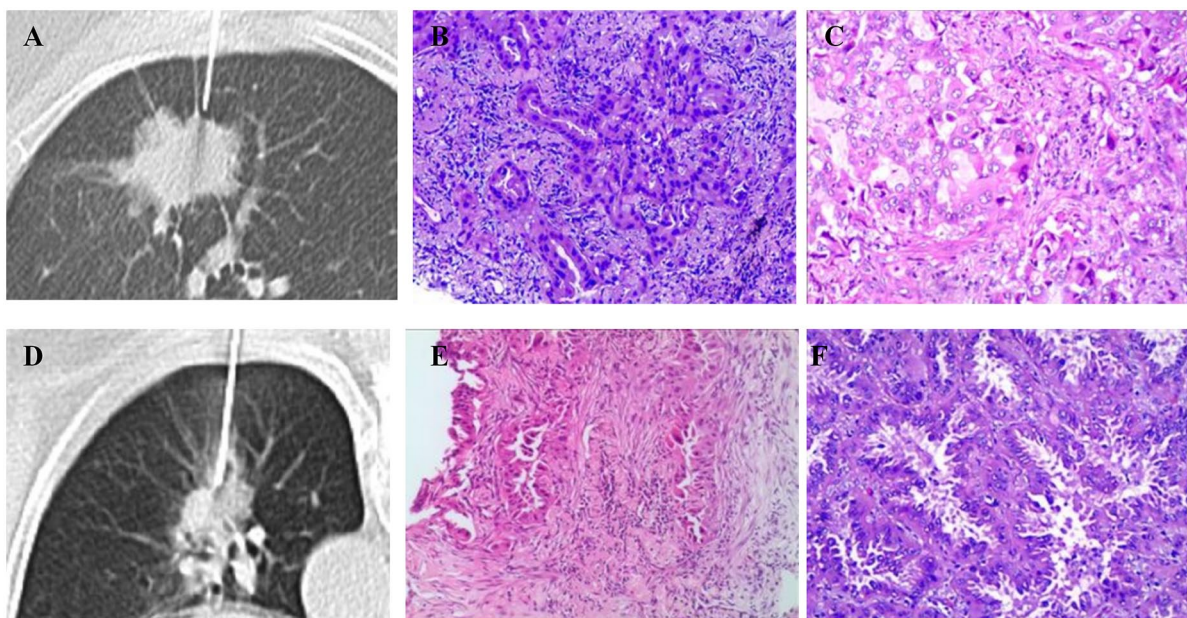

Figure 3. Grade inconsistency between biopsy and surgical specimen pathologies. Case 1, female, 69 years. Intraoperative route of biopsy needle (A); pathology results of the biopsy specimen show that, in this invasive lung adenocarcinoma, the ACI subtype accounted for 100% of the biopsy samples (B); pathology results of the surgical specimen show that in this invasive lung adenocarcinoma, the PAP subtype accounted for 50%, the ACI subtype accounted for 25%, and the SOL subtype accounted for 25% of the surgical samples (C). Case 2, female, 74 years. Intraoperative route of the biopsy needle (D); pathology results of the biopsy specimen shows that, in this invasive lung adenocarcinoma, the ACI subtype was predominant in the biopsy samples (E); the pathology results of the surgical specimen showed that, in this invasive lung adenocarcinoma, the ACI subtype accounted for 80% and the SOL subtype accounted for 20% of the surgical samples (F).
ACI indicates acinar; PAP, papillary; SOL, solid.

Our results showed that the specificity of poorly differentiated grade 3 was 100%, and the specificity of high-grade subtypes (MIP and SOL) was 99.2% and 99.1%, respectively. Grade 3 had a relatively low sensitivity (54.8%). In addition to the small sample size, another possible explanation for the low sensitivity of grade 3 is that high-grade subtypes are more likely to be degraded during the processing of biopsy tissue as compared with non-high-grade subtypes.[12] However, the PPV (100%) and accuracy (89.2%) of grade 3 tumors were relatively high. Similarly, a higher accuracy rate was found for MIP (98.5%) and SOL

(96.2%) than for LEP (81.5%), ACI (76.9%), and PAP (92.3%). As mentioned above, MIP subtypes and SOL subtypes have a poor prognosis, and grade 3 is poorly differentiated. This shows that preoperative CT-guided biopsy can accurately detect the subtypes with poor prognosis and judge the degree of differentiation in invasive non-mucinous lung adenocarcinoma, as well as provide a good basis of treatment selection.

According to the IASLC grading system for invasive non-mucinous lung adenocarcinoma, our results showed that the concordance rate between CT-guided biopsy histopathological

grade and surgical histopathological grade was 72.3% (94/130), and the concordance rate between CT-guided biopsy predominant histopathological subtype and predominant surgical histopathological subtype was 73.1% (95/130). This was similar to the finding of Kim et al.[12]

In addition to CT-guided biopsy, common preoperative methods for predicting histological subtypes are intraoperative frozen section and radial endobronchial ultrasound-guided bronchoscopic (R-EBUS); however, Yeh et al[13] showed that, when using intraoperative frozen section, it is difficult to predict the predominant pattern. Compared with CT-guided biopsy, R-EBUS had a lower accuracy in peripheral pulmonary lesions and a poor diagnostic rate for lung lesions less than 2 cm.[14] Even if the peripheral pulmonary lesions used by R-EBUS are combined with transbronchial biopsy (TBB), their specificity and sensitivity are lower than that for CT-guided percutaneous needle biopsy.[15] At present, the research focus also includes radiogenomics, that can identify epidermal growth factor receptor (EGFR) expression in lung cancer. Radiometrics combined with AI can distinguish lung adenocarcinoma from squamous cell carcinoma. However, no research has shown that genoradiomics can identify the specific subtypes of lung adenocarcinoma.

We investigated the factors that influenced the consistency of biopsy and surgical histopathological grading in the same patient. These factors included age, sex, imaging morphology, tumor size, biopsy specimen size, biopsy needle gauge, and pathological subtype of CT-guided biopsy. Age, sex, imaging morphology, tumor size, biopsy specimen size, and biopsy needle gauge did not affect the consistency of the pathological grading of both biopsy samples and surgical samples in the same patient. The pathological subtype of the CT-guided biopsy specimen was related to the consistency of the findings between the two systems. We further analyzed pathological subtypes obtained by CT-guided biopsy. Biopsy indicated that LEP was the main subtype, while surgical pathology showed that not-LEP subtypes were predominant. This suggests that we should be more careful in the diagnosis of LEP subtypes.

Our statistical analysis showed that in 130 patients with lung adenocarcinoma who underwent CT-guided biopsy, pneumothorax occurred in 19.2% (25/130). These pneumothoraxes were absorbed without special treatment, and no patient required chest tube insertion. This was similar to other reports stating that CT-guided biopsy had a low risk of complications.[16] Recent studies have shown that there was no correlation between percutaneous transthoracic needle biopsy and that there was an increase in the total recurrence and pleural recurrence in stage I lung cancer.[17] In percutaneous lung biopsy, only 6 out of 9783 biopsy data developed tumor seeding at the site of the biopsy route; among these, only 2 out of 6 biopsy data developed tumor seeding performed by the co-axial method.[18]

Our retrospective study had several limitations. First, the sample was small, and these samples were obtained from the same institution. In particular, the MIP and SOL predominant subtype samples accounted for 12.3% (16/130), whereas the ACI predominant subtype accounted for 64.6% (84/130)

according to surgical specimen-based pathology. Compared with the 40% to 50% ACI predominant subtype in other reports, our statistical results show a higher proportion of ACI predominant subtype. This may be because multiple pathologists were from the same institution, limiting the generalizability of the results.[19] Second, CT-guided percutaneous biopsy was performed by different interventional radiologists. The biopsy tissue and the complications of the biopsy procedure varies with different interventional radiologists. Third, the main difference in the grade is due to the differentiation of the LEP pattern versus the ACI pattern. We failed to find a high-grade pattern, particularly SOL patterns, in a biopsy sample (Table 5). The diagnostic differences between the LEP pattern and non-LEP pattern are emphasized by the American Joint committee on Cancer.[20] Therefore, more reliable methods that refine the definition of each pattern, as well as recognize other features (such as high-grade pattern) are needed.[4,21]

Conclusion

In summary, the present study showed that the preoperative CT-guided biopsy pathology grade is highly consistent with surgical pathology grade. It can predict the prognosis of invasive non-mucinous lung adenocarcinoma to a great extent, which may play an important role in deciding the therapy program before surgery. This study also showed that CT-guided percutaneous biopsy is a feasible and safe, minimally invasive technology for lung adenocarcinoma. Of course, to improve the accuracy of CT-guided biopsy pathology further, there is a need for larger sample populations, to elucidate the cause for the relatively low sensitivity of grade 3 in the grading system, to refine the definition of each pattern, and to recognize other features (such as high-grade patterns).

Author Contributions

Conceptualization: Dehao Liu and Lichun Chen.
Data collection: Xiaoping Wang, Yikai Lin and Jianwei Gu.
Statistical analysis: Lichun Chen.
Original draft: Dehao Liu and Lichun Chen.
Revised draft: All authors.

ORCID iD

Lichun Chen (iD) https://orcid.org/0000-0001-8144-3935

Supplemental Material

Supplemental material for this article is available online.

REFERENCES

1. Ferlay J, Colombet M, Soerjomataram I, et al. Estimating the global cancer incidence and mortality in 2018: GLOBOCAN sources and methods. *Int J Cancer*. 2019;144:1941-1953.
2. Zappa C, Mousa SA. Non-small cell lung cancer: current treatment and future advances. *Transl Lung Cancer Res*. 2016;5:288-300.
3. Travis WD, Brambilla E, Noguchi M, et al. International association for the study of lung cancer/American thoracic society/European respiratory society international multidisciplinary classification of lung adenocarcinoma. *J Thorac Oncol*. 2011;6:244-285.

4. Moreira AL, Ocampo PSS, Xia Y, et al. A grading system for invasive pulmonary adenocarcinoma: a proposal from the International Association for the Study of Lung Cancer Pathology Committee. *J Thorac Oncol*. 2020;15:1599-1610.

5. Travis WD, Brambilla E, Nicholson AG, et al.; WHO Panel. The 2015 World Health Organization classification of lung tumors: impact of genetic, clinical and radiologic advances since the 2004 classification. *J Thorac Oncol*. 2015;10: 1243-1260.

6. Tsao M. PL01.05 The new WHO classification of lung tumors. *J Thorac Oncol*. 2021;16:S63.

7. Mäkinen JM, Laitakari K, Johnson S, et al. Histological features of malignancy correlate with growth patterns and patient outcome in lung adenocarcinoma. *Histopathology*. 2017;71:425-436.

8. Kadota K, Kushida Y, Kagawa S, et al. Cribriform subtype is an independent predictor of recurrence and survival after adjustment for the eighth edition of TNM staging system in patients with resected lung adenocarcinoma. *J Thorac Oncol*. 2019;14:245-254.

9. Takahashi Y, Kuroda H, Oya Y, Matsutani N, Matsushita H, Kawamura M. Challenges for real-time intraoperative diagnosis of high-risk histology in lung adenocarcinoma: a necessity for sublobar resection. *Thorac Cancer*. 2019;10:1663-1668.

10. Gao S, Stein S, Petre EN, et al. Micropapillary and/or solid histologic subtype based on pre-treatment biopsy predicts local recurrence after thermal ablation of lung adenocarcinoma. *Cardiovasc Intervent Radiol*. 2018;41:253-259.

11. Leeman JE, Rimner A, Montecalvo J, et al. Histologic subtype in core lung biopsies of early-stage lung adenocarcinoma is a prognostic factor for treatment response and failure patterns after stereotactic body radiation therapy. *Int J Radiat Oncol Biol Phys*. 2017;97:138-145.

12. Kim TH, Buonocore D, Petre EN, et al. Utility of core biopsy specimen to identify histologic subtype and predict outcome for lung adenocarcinoma. *Ann Thorac Surg*. 2019;108:392-398.

13. Yeh YC, Nitadori J, Kadota K, et al. Using frozen section to identify histological patterns in stage I lung adenocarcinoma of ≤ 3 cm: accuracy and interobserver agreement. *Histopathology*. 2015;66:922-938.

14. Gupta A, Suri JC, Bhattacharya D, et al. Comparison of diagnostic yield and safety profile of radial endobronchial ultrasound-guided bronchoscopic lung biopsy with computed tomography-guided percutaneous needle biopsy in evaluation of peripheral pulmonary lesions: a randomized controlled trial. *Lung India*. 2018;35:9-15.

15. Steinfort DP, Khor YH, Manser RL, Irving LB. Radial probe endobronchial ultrasound for the diagnosis of peripheral lung cancer: systematic review and meta-analysis. *Eur Respir J*. 2011;37:902-910.

16. Patel JD. Overcoming perceived hurdles in lung cancer screening: the low risk of complications of image-guided transthoracic needle biopsy. *J Oncol Pract*. 2015;11:e360-e362.

17. Li H, Chen R, Zhao J. Correlation between percutaneous transthoracic needle biopsy and recurrence in stage I lung cancer: a systematic review and meta-analysis. *BMC Pulm Med*. 2020;20:198.

18. Tomiyama N, Yasuhara Y, Nakajima Y, et al. CT-guided needle biopsy of lung lesions: a survey of severe complication based on 9783 biopsies in Japan. *Eur J Radiol*. 2006;59:60-64.

19. Tsai PC, Yeh YC, Hsu PK, Chen CK, Chou TY, Wu YC. CT-guided core biopsy for peripheral sub-solid pulmonary nodules to predict predominant histological and aggressive subtypes of lung adenocarcinoma. *Ann Surg Oncol*. 2020;27:4405-4412.

20. Amin MB, Edge S, Greene F, et al. *AJCC Cancer Staging Manual*. 8th ed. New York, NY: Springer; 2017.

21. Shih AR, Uruga H, Bozkurtlar E, et al. Problems in the reproducibility of classification of small lung adenocarcinoma: an international interobserver study. *Histopathology*. 2019;75:649-659.